

Recent progress in pion photo- and electroproduction analysis

L. Tiator^a, D. Drechsel^a, S. Kamalov^b and S. N. Yang^c

^a*Institut für Kernphysik, Universität Mainz, 55099 Mainz, Germany*

^b*Laboratory of Theoretical Physics, JINR, 141980 Dubna, Russia*

^c*Department of Physics, National Taiwan University, Taipei, Taiwan*

(Received: November 14, 2018)

Pion photo- and electroproduction has been studied at threshold and in the resonance region below $W < 2$ GeV. At threshold π^0 production can be very well explained within a dynamical model derived from an effective chiral Lagrangian. The final state interaction is nearly saturated by single charge exchange rescattering. In the resonance region new electroproduction data at $Q^2 = 1$ GeV² has been analyzed with *MAID* and longitudinal and transverse photon helicity amplitudes have been determined for different resonances. A detailed study of the E/M and S/M ratios of the $N \rightarrow \Delta$ transition shows a zero crossing of R_{EM} near $Q^2 = 4$ GeV², whereas the R_{SM} becomes increasingly negative at large Q^2 .

1 Introduction

The unitary isobar model *MAID* is a model for single pion photo- and electroproduction off protons and neutrons [1]. It is based on a non-resonant background described by Born terms and vector meson exchange contributions and nucleon resonance excitations modeled by Breit-Wigner functions

$$t_{\gamma\pi}^\alpha = t_{\gamma\pi}^{B,\alpha} + t_{\gamma\pi}^{R,\alpha}. \quad (1)$$

Both parts, background and resonance are separately unitarized. This has been achieved by a K-matrix unitarization in the case of the background

$$t_{\gamma\pi}^{B,\alpha}(MAID) = \exp(i\delta_\alpha) \cos \delta_\alpha v_{\gamma\pi}^{B,\alpha}(W, Q^2), \quad (2)$$

and by introducing a unitary phase ϕ_R for the resonance excitations

$$t_{\gamma\pi}^{R,\alpha}(W, Q^2) = \bar{\mathcal{A}}_\alpha^R(Q^2) \frac{f_{\gamma R}(W) \Gamma_R M_R f_{\pi R}(W)}{M_R^2 - W^2 - i M_R \Gamma_R} e^{i\phi_R}. \quad (3)$$

The phases δ_α are the elastic pion-nucleon scattering phases in a particular channel $\alpha = \{l, j, t\}$ below the inelastic threshold of two-pion production. In order to take account of inelastic effects, the factor $\exp(i\delta_\alpha) \cos \delta_\alpha$ is replaced by $\frac{1}{2}[\eta_\alpha \exp(2i\delta_\alpha) + 1]$ with the inelasticity parameters η_α at higher energies. Additional background terms are included to account for S- and P-wave pion loop effects.

In the case of the Dynamical Model (*DMT*) [2], the background contribution is given by

$$t_{\gamma\pi}^{B,\alpha}(DMT) = e^{i\delta_\alpha} \cos \delta_\alpha \left[v_{\gamma\pi}^{B,\alpha} + P \int_0^\infty dq' \frac{q'^2 R_{\pi N}^{(\alpha)}(q, q') v_{\gamma\pi}^{B,\alpha}(q')}{W - E_{\pi N}(q')} \right] \quad (4)$$

with the full πN scattering reaction matrix $R_{\pi N}^{(\alpha)}$. In this case the pion loop effects that are especially important near threshold are generated dynamically and show up as a principal value integral over the reaction matrix.

Presently, we have included 8 nucleon resonances, 3 Deltas: $P_{33}(1232)$, $S_{31}(1620)$ and $D_{33}(1700)$ and 5 N^* s: $P_{11}(1440)$, $D_{13}(1520)$, $S_{11}(1535)$, $S_{11}(1650)$ and $F_{15}(1680)$. All of them are included with longitudinal and transverse electromagnetic couplings. The corresponding helicity amplitudes $A_{1/2}$, $A_{3/2}$ and $S_{1/2}$ can be fitted to experimental data and can be freely changed in the *MAID* program.

We will show results obtained with the Dynamical Model for the threshold region and present some recent fits to newer electroproduction data with *MAID* for the resonance region with a discussion of the Q^2 evolution of the E/M and S/M ratios of the $N \rightarrow \Delta(1232)$ transition.

2 Results in the threshold region

For π^0 photoproduction, we first calculate the multipole E_{0+} near threshold by solving the coupled channels equation within a basis with physical pion and nucleon masses. The coupled channels equation leads to the following expression for the pion photoproduction t-matrix in the $\pi^0 p$ channel:

$$\begin{aligned} t_{\gamma\pi^0}(W) &= v_{\gamma\pi^0}(W) + v_{\gamma\pi^0}(W) g_{\pi^0 p}(W) t_{\pi^0 p \rightarrow \pi^0 p}(W) \\ &+ v_{\gamma\pi^+}(W) g_{\pi^+ n}(W) t_{\pi^+ n \rightarrow \pi^0 p}(W), \end{aligned} \quad (5)$$

where $t_{\pi^0 p \rightarrow \pi^0 p}$ and $t_{\pi^+ n \rightarrow \pi^0 p}$ are the πN t-matrices in the elastic and charge exchange channels, respectively. They are obtained by solving the coupled channels equation for πN scattering using the meson-exchange model of Ref. [3]. Our results for $Re E_{0+}$ show that practically all of the final state interaction effects originate from the $\pi^+ n$ channel and mainly stems from the principal value integral of Eq. (5). In this approach the $t_{\pi N}$ matrix contains the effect of πN rescattering to all orders. However, we have indeed found that only the first order rescattering contribution, i.e. the one-loop diagram, is important. This indicates that the one-loop calculation in ChPT is a reliable approximation for π^0 production in the threshold region.

If the FSI effects are evaluated with the assumption of isospin symmetry (IS), i.e., with averaged masses in the free pion-nucleon propagator, the energy dependence in $Re E_{0+}$ in the threshold region is very smooth. Below π^+ threshold the strong energy dependence (cusp effect) [4] only appears because of the pion mass difference and, as we have seen above, is related to the coupling with the $\pi^+ n$ channel. In most calculations, the effects from the pion mass difference below the π^+ production channel are taken into account by using the K-matrix approach [5],

$$Re E_{0+}^{\gamma\pi^0} = Re E_{0+}^{\gamma\pi^0}(IS) - a_{\pi N} \omega_c Re E_{0+}^{\gamma\pi^+}(IS) \sqrt{1 - \frac{\omega^2}{\omega_c^2}}, \quad (6)$$

where ω and ω_c are the π^0 and π^+ c.m. energies corresponding to $W = E_p + \omega_\gamma$ and $m_n + m_{\pi^+}$, respectively, and $a_{\pi N} = 0.124/m_{\pi^+}$ is the pion charge exchange threshold amplitude. $E_{0+}^{\gamma\pi^{0,+}}(IS)$ is the $\pi^{0,+}$ photoproduction amplitude obtained with the assumption of isospin symmetry (IS), i.e., without the pion mass difference in Eq. (4). Such an approximation is often used in the data analysis in order to parametrize the E_{0+} multipole below $\pi^+ n$ threshold in the form of $E_{0+}(E) = a + b\sqrt{1 - (\omega/\omega_c)^2}$. Numerically this approximation is very precise and differs only by 10% at the π^0 threshold and becomes indistinguishable above the π^+ threshold. In Fig. 1 the results obtained within this approximation scheme are represented by the solid curve and compared to the ChPT calculation (dash-dotted curve) [6]. Over the whole energy range the difference is rather small and within the experimental uncertainties. Huge effects, however, arise if the cusp would be neglected or obviously if the FSI effects would be totally ignored (dotted curve).

In Fig. 1 we also compare the predictions of our model for the differential cross section with recent photoproduction data from Mainz [8,9]. The dotted and solid curves are obtained without and

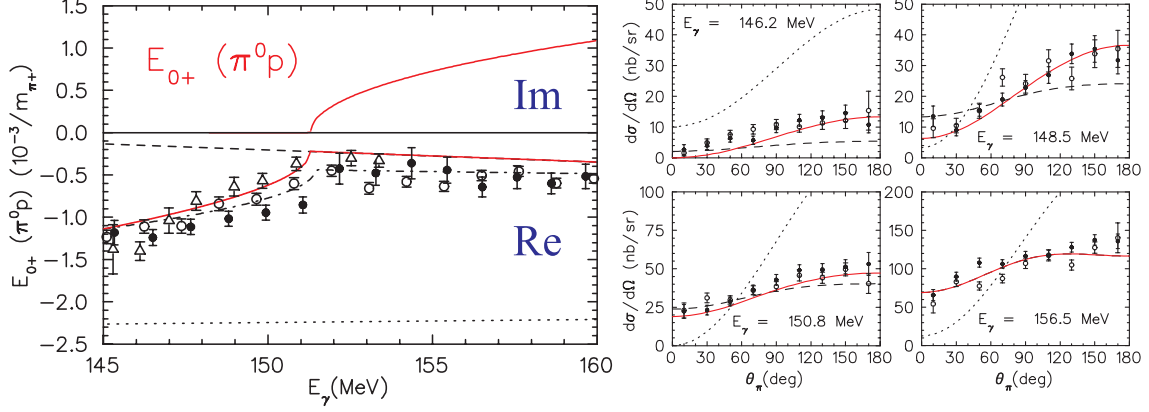


Figure 1: Real and imaginary parts of the E_{0+} multipole and differential cross sections below and above π^+ threshold for $\gamma p \rightarrow \pi^0 p$. The solid and dashed curves obtained with and without the cusp effect, respectively. The dotted curve is without FSI. The dash-dotted curve is the result of ChPT [5]. Data points for E_{0+} from Mainz [8](\triangle), [9](\circ) and Saskatoon [10](\bullet), and for $d\sigma$ from Mainz [8](\bullet), [9](\circ).

with FSI effects, respectively. It is seen that both off-shell pion rescattering and cusp effect substantially improve the agreement with the data. This indicates that our model gives reliable predictions also for the threshold behaviour of the P -waves without any additional arbitrary parameters.

Pion electroproduction provides us with information on the $Q^2 = -k^2$ dependence of the transverse E_{0+} and longitudinal L_{0+} multipoles in the threshold region. The "cusp" effects in the L_{0+} multipole is taken into account in a similar way as in the case of E_{0+} ,

$$Re L_{0+}^{\gamma\pi^0} = Re L_{0+}^{\gamma\pi^0}(IS) - a_{\pi N} \omega_c Re L_{0+}^{\gamma\pi^+}(IS) \sqrt{1 - \frac{\omega^2}{\omega_c^2}}, \quad (7)$$

where all the multipoles are functions of total c.m. energy W and virtual photon four-momentum squared Q^2 . It is known that at threshold, the Q^2 dependence is given mainly by the Born plus vector meson contributions in $v_{\gamma\pi}^B$, as described in Ref. [1]. Similar to pion photoproduction, the K-matrix approximation and full calculation agree with each other within a few percent. In Fig. 2 we show our results for the cusp and FSI effects in the E_{0+} and L_{0+} multipoles for π^0 electroproduction at $Q^2 = 0.1$ (GeV/c) 2 , along with the results of the multipole analysis from NIKHEF [11] and Mainz [12]. Note that results of both groups were obtained using the P -wave predictions given by ChPT. However, there exist substantial differences between the P -wave predictions of ChPT and our model at finite Q^2 . To understand the consequence of these differences, we have made a new analysis of the Mainz data [12] for the differential cross sections, using our *DMT* prediction for the P -wave multipoles instead. The S -wave multipoles extracted this way are also shown in Fig. 2 by solid circles. We see that the results of such a new analysis gives E_{0+} multipoles closer to the NIKHEF data and in better agreement with our dynamical model prediction. However, the results of our new analysis for the longitudinal L_{0+} multipoles stay practically unchanged from the values found in the previous analyses. Note that the dynamical model prediction for L_{0+} again agrees much better with the NIKHEF data. Further details are given in Ref. [13]

In contrast to *DMT*, in *MAID* the FSI effects are taken into account using the K-matrix approximation, namely without the inclusion of off-shell pion rescattering contributions (principal value integral) in Eq. (4). As a result, the S -, P -, D - and F -waves of the background contributions

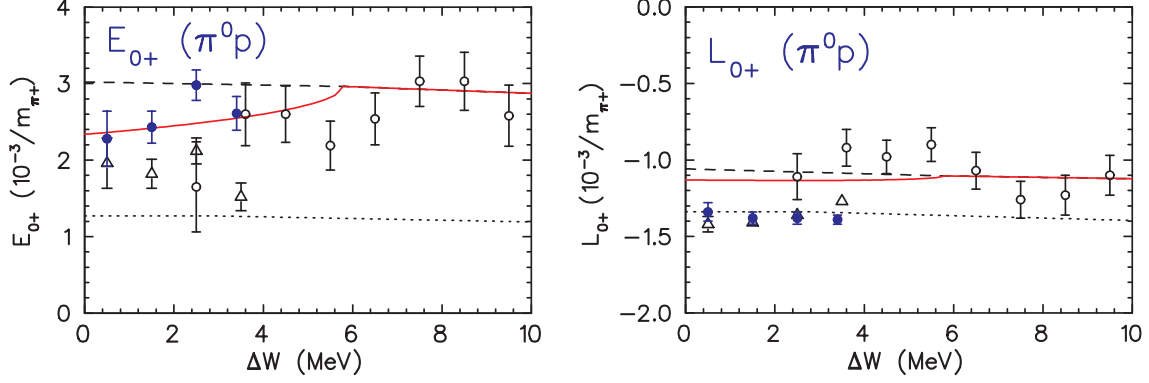


Figure 2: Real parts of E_{0+} and L_{0+} for $ep \rightarrow e'\pi^0 p$ at $Q^2=0.1$ (GeV/c) 2 . Notations are the same as in Fig. 1. Data points from NIKHEF [11](\circ) and Mainz [12](\triangle). The results of the present work obtained by using the P -waves of our model are given by (\bullet).

are defined as

$$t_{\alpha}^B(MAID) = \exp(i\delta_{\alpha}) \cos \delta_{\alpha} v_{\alpha}^B(q_E, k). \quad (8)$$

However, as we have found above, dynamical model calculations show that pion off-shell rescattering is very important at low pion energies. The prediction of *MAID* for $E_{0+}(\pi^0 p)$ at threshold, represented by the dotted curves in Fig. 1 lies substantially below the data. It turns out that it is possible to improve *MAID*, in the case of π^0 production at low energies, by introducing a phenomenological term and including the cusp effect of Eq. (6). In this extended version of *MAID2000*, we write the $E_{0+}(\pi^0 p)$ multipole as

$$Re E_{0+}^{\gamma\pi^0} = Re E_{0+}^{\gamma\pi^0}(MAID98) + E_{cusp}(W, Q^2) + E_{corr}(W, Q^2), \quad (9)$$

where

$$E_{cusp}(W, Q^2) = -a_{\pi N} \omega_c Re E_{0+}^{\gamma\pi^+}(MAID98) \sqrt{1 - \frac{\omega^2}{\omega_c^2}}. \quad (10)$$

The phenomenological term E_{corr} which emulates the pion off-shell rescattering corrections (or pion-loop contribution in ChPT) can be parameterized in the form

$$E_{corr}(W, Q^2) = \frac{A}{(1 + B^2 q_{\pi}^2)^2} F_D(Q^2), \quad (11)$$

where F_D is the standard nucleon dipole form factor. The parameters A and B are obtained by fitting to the low energy π^0 photoproduction data: $A = 2.01 \times 10^{-3}/m_{\pi^+}$ and $B = 0.71 fm$.

3 Results in the resonance region

For pion photoproduction in the resonance region we have recently performed a fit of *MAID* for both the low-energy Δ region and the medium-energy resonance region up to $W = 1700$ MeV, where resonance parameters have been obtained as a part of the BRAG¹ partial wave benchmark analysis [14]. In Fig. 3 we present a new fit of preliminary results on electroproduction, $p(e, e'p)\pi^0$,

¹Baryon Resonance Analysis Group, <http://cnr2.kent.edu/~manley/BRAG.html>

measured by the JLab Hall A collaboration [15]. The data has been taken at backward angles at $Q^2 = 1.0 \text{ GeV}^2$ in the c.m. energy range from 0.95 GeV to 2.0 GeV. With a dataset of 363 data points in 3 observables, $d\sigma = d\sigma_T + \epsilon d\sigma_L$, $d\sigma_{LT}$ and $d\sigma_{TT}$ and pion angles of 146, 151 and 167 degrees we performed a data analysis with *MAID*.

From the 20 possible resonance parameters we have varied 18 by fixing E_{2-} and S_{2-} of the $D_{13}(1520)$ because we did not find enough sensitivity in the data which are only taken at backward angles. In table 1 we give the result of our fit both for the multipole and the helicity amplitudes. The multipole amplitudes are compared to the default values of *MAID*. For the $\Delta(1232)$ resonance we give in addition the E/M and the S/M ratios. Both are consistent with the previous *MAID* fits to photo- and electroproduction [16]. The R_{SM} ratio is very well determined by the $d\sigma_{LT}$ data and shows the tendency to larger negative values for increasing Q^2 , while the R_{EM} ratio is much more uncertain and also the model uncertainties are larger than for the S/M ratio. From $d\sigma_{LT}$ we also find a large sensitivity to the S_{0+} amplitude of the $S_{11}(1535)$ resonance in the minimum around $W = 1500 \text{ MeV}$ as well as for the S_{2-} amplitude of the $D_{33}(1700)$ resonance in the second maximum around $W = 1650 \text{ MeV}$. Furthermore most of the structure in $d\sigma$ and in $d\sigma_{TT}$ above $W = 1700 \text{ MeV}$ is explained by the M_{2-} amplitude of the $D_{33}(1700)$ resonance. However, the *MAID* model does not include higher resonances so far.

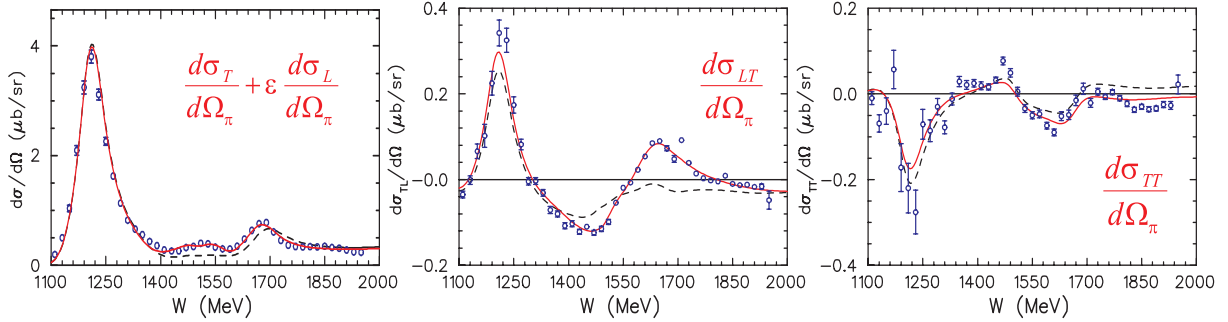


Figure 3: Preliminary experimental results from the JLab Hall A collaboration [15] at $Q^2 = 1.0 \text{ GeV}^2$, $\theta_\pi = 167^\circ$ and $\epsilon = 0.9$ as functions of the c.m. energy W . The dashed lines show the standard *MAID*2000 calculations and the solid curves are the results of the fit to the data.

In order to get information on resonance properties a careful analysis has to be taken. First of all, a partial wave decomposition in terms of multipoles is necessary to get information on quantum numbers as angular momentum, spin, parity and isospin. Second, a background separation is needed, as especially in pion production a large background is produced by the strong pion nucleon coupling. However, nucleon Born terms and vector meson exchange contributions are not the only source of background. Loop effects can give very large contributions especially for S- and P-waves, the most famous example is the E_{0+} in π^0 photoproduction at threshold. Our resonance extraction is based on the imaginary parts of the full multipoles in a specific spin-isospin channel at the resonance position. This minimizes the model dependence since resonance positions are mostly well known and this method can be applied to any given partial wave analysis. It is very similar to the method that has been applied for the $\Delta(1232)$, however, as Watson's theorem is no longer fulfilled for higher resonances, some uncertainties have to be accepted. The helicity amplitudes extracted by this way are “dressed” amplitudes and contain contributions from vertex corrections. They could be undressed by subtracting background contributions and unitarization corrections. By such a procedure they could be directly related to the Breit-Wigner couplings $\bar{\mathcal{A}}_\alpha^R(Q^2)$ of Eq. (3), however, such a method will always be model dependent.

The helicity amplitudes $A_{1/2}$, $A_{3/2}$ and $S_{1/2}$ are determined from the pion electroproduction

multipoles at the resonance position

$$A_{1/2}^{\ell+} = -\frac{1}{2ac_I}[(\ell+2)\tilde{E}_{\ell+} + \ell\tilde{M}_{\ell+}] \quad (12)$$

$$A_{1/2}^{(\ell+1)-} = +\frac{1}{2ac_I}[(\ell+2)\tilde{M}_{(\ell+1)-} - \ell\tilde{E}_{(\ell+1)-}] \quad (13)$$

$$A_{3/2}^{\ell+} = +\frac{1}{2ac_I}\sqrt{\ell(\ell+2)}[\tilde{E}_{\ell+} - \tilde{M}_{\ell+}] \quad (14)$$

$$A_{3/2}^{(\ell+1)-} = -\frac{1}{2ac_I}\sqrt{\ell(\ell+2)}[\tilde{E}_{(\ell+1)-} + \tilde{M}_{(\ell+1)-}] \quad (15)$$

$$S_{1/2}^{\ell+} = -\frac{1}{\sqrt{2}ac_I}(\ell+1)\tilde{S}_{\ell+} \quad (16)$$

$$S_{1/2}^{(\ell+1)-} = -\frac{1}{\sqrt{2}ac_I}(\ell+1)\tilde{S}_{(\ell+1)-} \quad (17)$$

$$\text{with } a = \sqrt{\frac{1}{\pi} \frac{k_W^R}{q_\pi^R} \frac{1}{2J+1} \frac{m_N}{M_R} \frac{\Gamma_\pi}{\Gamma_{tot}^2}} \quad \text{and} \quad c_I = \begin{cases} -\sqrt{1/3} & : I = 1/2 \\ \sqrt{3/2} & : I = 3/2 \end{cases} \quad (18)$$

The equivalent photon energy k_W^R and the pion momentum q_π^R are given in the c.m. frame and evaluated at the resonance position, where also the pion electroproduction multipoles are obtained, $\tilde{A} \equiv \text{Im}A(W = M_R)$ for $A = E, M, S$. For the transverse amplitudes these formulas agree with PDG and Ref. [17]. For longitudinal amplitudes we found different definitions in the literature, here we use a definition consistent with notations used in DIS [18].

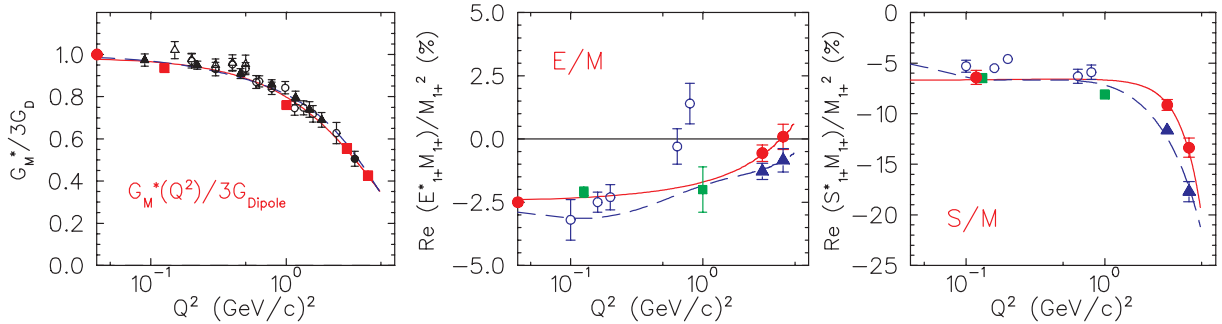


Figure 4: The Q^2 dependence of the magnetic G_M^* form factor and the E/M and S/M ratios at $W = 1232$ MeV. The solid and dashed curves are the *MAID* and dynamical model results, respectively. JLab results discussed here are shown at $Q^2 = 1$ (GeV/c) 2 , Bates results at 0.126 (squares), the Mainz double polarization result of S/M at 0.12 (full circle), data at 2.8 and 4.0 from Ref. [19] (squares) and preliminary results of the ratios in the range of 0.1 - 0.8 are from Bonn [20] (open circles). Results of our analysis for the ratios at 2.8 and 4.0 are obtained using *MAID* (full circles) and the dynamical models (triangles). In the case of G_M^* they fully agree with Ref. [19]. For older data of G_M^* see Ref. [16]. The photoproduction results of Mainz [21] are placed at the lowest Q^2 value. All numbers are given in units of (GeV/c) 2 .

In Fig. 4 we show our extracted values for the magnetic form factor $G_M^*/3G_D$ and the ratios R_{EM} and R_{SM} together with other data determined in different ways in recent experiments and data analyses on a semi-log scale. For photoproduction the Mainz results [21] are shown, around 0.125 GeV 2 the values of the Bates analysis and the result of the Mainz measurement with recoil

N^*		<i>MAID</i> defaults	<i>MAID</i> fit results	helicity amplitudes	
$P_{33}(1232)$	$\tilde{E}_{1+}^{3/2}$	-0.44	-0.38 ± 0.17	$A_{1/2}$	-72 ± 3
	$\tilde{M}_{1+}^{3/2}$	20.1	19.0 ± 0.4	$A_{3/2}$	-135 ± 3
	$\tilde{S}_{1+}^{3/2}$	-1.31	-1.55 ± 0.05	$S_{1/2}$	18 ± 1
	R_{EM}	-2.2	-2.0 ± 0.9		
	R_{SM}	-6.5	-8.1 ± 0.2		
$P_{11}(1440)$	$\tilde{M}_{1-}^{1/2}$	1.87	2.2 ± 0.2	$A_{1/2}$	-59 ± 9
	$\tilde{S}_{1-}^{1/2}$	1.26	0.6 ± 0.1	$S_{1/2}$	-11 ± 4
$D_{13}(1520)$	$\tilde{E}_{2-}^{1/2}$	-0.05	-0.05	$A_{1/2}$	-47 ± 6
	$\tilde{M}_{2-}^{1/2}$	1.71	1.2 ± 0.2	$A_{3/2}$	26 ± 4
	$\tilde{S}_{2-}^{1/2}$	0	0	$S_{1/2}$	0
$S_{11}(1535)$	$\tilde{E}_{0+}^{1/2}$	4.37	3.5 ± 0.8	$A_{1/2}$	61 ± 14
	$\tilde{S}_{0+}^{1/2}$	0.1	-1.2 ± 0.1	$S_{1/2}$	-15 ± 2
$S_{31}(1620)$	$\tilde{E}_{0+}^{3/2}$	0.21	3.4 ± 0.3	$A_{1/2}$	-50 ± 5
	$\tilde{S}_{0+}^{3/2}$	0.89	1.7 ± 0.5	$S_{1/2}$	-18 ± 7
$S_{11}(1650)$	$\tilde{E}_{0+}^{1/2}$	2.8	3.0 ± 0.4	$A_{1/2}$	43 ± 6
	$\tilde{S}_{0+}^{1/2}$	0	-1.2 ± 0.6	$S_{1/2}$	-12 ± 6
	$\tilde{E}_{0+}^{3/2}$	0.32	-0.06 ± 0.03	$A_{1/2}$	-52 ± 9
$F_{15}(1680)$	$\tilde{M}_{3-}^{1/2}$	0.83	0.80 ± 0.05	$A_{3/2}$	33 ± 9
	$\tilde{S}_{3-}^{1/2}$	0	-0.10 ± 0.03	$S_{1/2}$	-7 ± 2
	$\tilde{E}_{2-}^{3/2}$	-0.85	-1.0 ± 0.2	$A_{1/2}$	104 ± 12
$D_{33}(1700)$	$\tilde{M}_{2-}^{3/2}$	0.30	1.1 ± 0.1	$A_{3/2}$	-4 ± 12
	$\tilde{S}_{2-}^{3/2}$	0	0.2 ± 0.1	$S_{1/2}$	-14 ± 7
PV-PS mixing:	Λ_m	450	350 ± 35		

Table 1: Proton resonance multipoles ($\tilde{A} \equiv \text{Im}A(W = M_r)$ in $10^{-3}/m_\pi$), helicity amplitudes (in $10^{-3} \text{ GeV}^{-1/2}$) and values of the PV-PS mixing parameter Λ_m (in MeV) as in *MAID*2000 and obtained in our fit at $Q^2 = 1.0 \text{ GeV}^2$. The $D_{13}(1520)$ \tilde{E}_{2-} and \tilde{S}_{2-} amplitudes were fixed. The E/M and S/M ratios of the $\Delta(1232)$ are given in percentage.

polarization, in the medium Q^2 range the preliminary data of Bonn [20] and at high Q^2 our analysis of the JLab Hall C data [19] with *MAID* and the *DMT*. The main difference between our results and those of Ref. [19] is that our values of R_{EM} show a clear tendency to cross zero and change sign as Q^2 increases. This is in contrast with the results obtained in the original analysis [19] of the data which concluded that R_{EM} would stay negative and tend toward more negative values with increasing Q^2 . Furthermore, we find that the absolute value of R_{SM} is strongly increasing.

4 Summary

With the unitary isobar model *MAID* and the dynamical model *DMT* we have two very good tools available to analyze data of pion photo- and electroproduction and to plan new experiments with increased sensitivity to specific questions. While *DMT* includes pion loop contributions that are especially important for low partial waves (S and P), *MAID* originally was constructed only from tree diagrams, resonance excitations and K-matrix unitarization contributions. Therefore, to get better agreement for S-waves, *MAID* has been extended phenomenologically by low-energy corrections and the unitary cusp effect. At higher energies the PS-PV mixing of *MAID* that was already introduced from the beginning, also serves for this purpose to effectively taking into account of loop contributions.

With all parameters already fixed by πN scattering and pion photoproduction in the resonance

region, *DMT* describes pion photoproduction at threshold very well, similar to the calculations in ChPT or with dispersion relations. For electroproduction at threshold we also find good agreement with the experiment at $Q^2 = 0.1 \text{ GeV}^2$, however, we also have problems describing the recent Mainz data at $Q^2 = 0.05 \text{ GeV}^2$ as it also appears in ChPT calculations. In the resonance region both models *DMT* and *MAID* can equally well describe photo- and electroproduction data up to $W = 1700 \text{ MeV}$ by fitting the photon helicity amplitudes $A_{1/2}$, $A_{3/2}$ and $S_{1/2}$ of the individual resonances. Here, we have demonstrated this with the preliminary Hall A data of JLab at $Q^2 = 1.0 \text{ GeV}^2$. Even with a dataset limited to backward pion angles we are able to determine quite a few resonance parameters in satisfactory precision and can also give longitudinal couplings where previous information practically did not exist. For the E/M and S/M ratios of the Delta resonance we combine our previous fits of Mainz, Bates and JLab Hall C data with our new analysis and find a consistent Q^2 evolution of these ratios with a slowly rising R_{EM} that crosses zero around $Q^2 = 4 \text{ GeV}^2$, and for the longitudinal coupling a R_{SM} that significantly increases to larger negative values at high Q^2 . If expectations from pQCD will be fulfilled, a sharp rise in the E/M ratio towards 100% should be seen in the next generation of experiments above $Q^2 = 5 \text{ GeV}^2$ and a leveling of the S/M ratio to a constant value.

Acknowledgments: We gratefully acknowledge financial support of this work in parts by the National Science Council of ROC under Grant No. NSC89-2112-M002-078, by Deutsche Forschungsgemeinschaft (SFB 443), and by a joint project NSC/DFG TAI-113/10/0.

References

- [1] D. Drechsel, O. Hanstein, S.S. Kamalov and L. Tiator, Nucl. Phys. **A645**, 145 (1999); in the internet at <http://www.kph.uni-mainz.de/MAID/>.
- [2] S.S. Kamalov and S.N. Yang, Phys. Rev. Lett. **83**, 4494 (1999); S.N. Yang, J. Phys. G **11**, L205 (1985).
- [3] C.T. Hung, S. N. Yang, and T.-S.H. Lee, J. Phys. G **20**, 1531 (1994); Phys. Rev. C **64**, 034309 (2001).
- [4] A. M. Bernstein, Phys. Lett. B **442**, 20 (1998).
- [5] V. Bernard, N. Kaiser, and Ulf-G. Meißner, Z. Phys. C **70** (1996) 483; Nucl. Phys. A **607**, 379 (1996); and references contained therein.
- [6] V. Bernard, J. Gasser, N. Kaiser, and Ulf-G. Meißner, Phys. Lett. B **268**, 291 (1991).
- [7] J. M. Laget, Phys. Rep. **69**, 1 (1981).
- [8] M. Fuchs *et al.*, Phys. Lett. B **368**, 20 (1996).
- [9] A. Schmidt *et al.*, nucl-exp/0105010, Phys. Rev. Lett. (2001) in print.
- [10] J. C. Bergstrom *et al.*, Phys. Rev. C **53**, R1052 (1996); C **55**, 2016 (1997).
- [11] H. B. van den Brink *et al.*, Phys. Rev. Lett. **74**, 3561 (1995); Nucl. Phys. A **612**, 391 (1997).
- [12] M. O. Distler *et al.*, Phys. Rev. Lett. **80**, 2294 (1998).
- [13] S.S. Kamalov, G.-Y. Chen, S.N. Yang, D. Drechsel and L. Tiator, nucl-th/0107017, Phys. Lett. B in print.
- [14] R.A. Arndt, I. Aznauryan, R.M. Davidson, D. Drechsel, O. Hanstein, S.S. Kamalov, A.S. Omelaenko, I. Strakovsky, L. Tiator, R.L. Workman, S.A.N. Yang, Proc. of NSTAR2001, Mainz, World Scientific 2001, p 467.
- [15] G. Laveissiere *et al.*, Proc. of NSTAR2001, Mainz, World Scientific 2001, p 271.
- [16] S.S. Kamalov, S.N. Yang, D. Drechsel, O. Hanstein, and L. Tiator, Phys. Rev. C **64**, 032201 (2001).
- [17] R.A. Arndt *et al.*, Phys. Rev. C **42**, 1864 (1990).
- [18] K. Abe *et al.*, Phys. Rev. D **58**, 112003 (1998).
- [19] V.V. Frolov *et al.*, Phys. Rev. Lett. **82**, 45 (1999).
- [20] R.W. Gothe, Prog. Part. Nucl. Phys. **44**, 185 (2000).
- [21] R. Beck *et al.* Phys. Rev. Lett. **78**, 606 (1997).